Research Square

Preprints are preliminary reports that have not undergone peer review.
They should not be considered conclusive, used to inform clinical practice,
or referenced by the media as validated information.

Electrospun poly(ε-caprolactone) mats containing sitophilure and activated carbon: thermal characterization and release-related behavior

Clara Andrezza Crisóstomo Bezerra Costa
Federal University of Alagoas (UFAL)
Ligia Maria Manzine Costa
São Paulo State University (UNESP)
João Gomes Costa
Embrapa Food and Territories
Alan John Duarte Freitas
Federal Institute of Alagoas (IFAL)
Henrique Fonseca Goulart
Federal University of Alagoas (UFAL)
Antônio Euzébio Goulart Sant'Anna
Federal University of Alagoas (UFAL)
Johnnatan Duarte Freitas
johnnatan.duarte@ifal.edu.br
Federal Institute of Alagoas (IFAL)

Research Article

Keywords: Electrospinning. Poly(ε-caprolactone). Aggregation pheromone. Sitophilus zeamais. Controlled release kinetics

Posted Date: November 27th, 2026

DOI: https://doi.org/10.21203/rs.3.rs-11473017/v1

License: This work is licensed under a Creative Commons Attribution 4.0 International License.
Read Full License

Additional Declarations: No competing interests reported.

Electrospun poly(ε-caprolactone) mats containing sitophilure and activated carbon: thermal characterization and release-related behavior

Clara Andrezza Crisóstomo Bezerra Costa[1,2*]. Ligia Maria Manzine Costa[3]. João Gomes da Costa[4]. Alan John Duarte de Freitas[1], Henrique Fonseca Goulart[2]. Antônio Euzébio Goulart Sant'Anna[2]. Johnnatan Duarte de Freitas[1]

[1]Multi-User Laboratory of Environmental Technologies (LMTA), Graduate Program in Environmental Technologies (PPGTEC), Federal Institute of Alagoas (IFAL), Maceió, Alagoas, 57020-600, Brazil.
Email: dra.clarapesquisa@gmail.com*
[2]Laboratory of Research in Natural Resources (LPRN), Institute of Chemistry and Biotechnology, Federal University of Alagoas (UFAL), Maceió, Alagoas, 57072-970, Brazil.
[3]Laboratory of Biomaterials of the Department of Physics and Chemistry at the São Paulo State University (UNESP), Ilha Solteira, São Paulo, 15385-007, Brazil.
[4]Embrapa Food and Territories, Maceió, Alagoas, 57020-050, Brazil.

Abstract
The development of biodegradable controlled-release systems for agricultural pest management represents a promising strategy for improving the retention of volatile active compounds. In this study, the aggregation pheromone sitophilure was synthesized via aldol addition (60.3% yield) and characterized by $^{1}H/^{13}C$ NMR, GC-MS, and FTIR-ATR. The compound was subsequently incorporated into electrospun poly(ε-caprolactone) (PCL) mats with and without activated carbon to investigate their physicochemical properties, thermal behavior, apparent release kinetics, and biological activity against *Sitophilus zeamais*. The formulations were characterized by TGA, DSC, FTIR-ATR, SEM, swelling tests, isothermal TGA, and Y-tube olfactometer bioassays. Thermogravimetric analysis showed that neat sitophilure exhibited substantial mass loss below 200 °C, whereas the PCL-based formulations displayed greater overall mass retention. FTIR-ATR analysis indicated preservation of the characteristic chemical structure of PCL after incorporation of the active compound. SEM micrographs revealed continuous electrospun fibers with activated carbon particles distributed on their surfaces. Swelling tests demonstrated increased water uptake, reaching a mean value of 422.1 ± 162.5% for PCL/sitophilure under acidic conditions. Isothermal TGA revealed temperature- and formulation-dependent mass-loss profiles, which were empirically described using the Korsmeyer–Peppas model. Because unloaded-matrix controls were unavailable, the normalized gravimetric response was interpreted as apparent release-related behavior rather than direct quantification of sitophilure release. Y-tube olfactometer bioassays demonstrated statistically significant attraction of *S. zeamais* to sitophilure-loaded mats ($p < 0.001$). Overall, the findings highlight the potential of electrospun PCL-based formulations as biodegradable carriers for volatile semiochemicals in agricultural pest management.

Keywords: Electrospinning. Poly(ε-caprolactone). Aggregation pheromone. *Sitophilus zeamais*. Controlled release kinetics.

1. Introduction

The maize weevil (*Sitophilus zeamais*), belonging to the order Coleoptera and the family Curculionidae, represents an important agricultural pest, causing significant economic losses by attacking the grains both in the pre-harvest phase and during storage [1, 2]. This species causes rapid loss of mass and depreciation of the commercial quality of corn grains. Its life cycle lasts approximately 37 days, and each female can lay about 150 eggs during this period [3].

Historically, the control of these pests has relied on the use of chemical insecticides, including organochlorine, organophosphate, and pyrethroid compounds. However, the intensive use of these products may be associated with the selection of resistant populations and the presence of residues in stored products, which has stimulated the search for more sustainable strategies [4]. Among these alternatives, physical control methods stand out, such as thermal management, the use of controlled atmospheres, and the application of diatomaceous earth; biological control, with the use of entomopathogenic fungi like *Beauveria bassiana* [5] and the use of semiochemicals, especially pheromones, as monitoring and control tools within the scope of Integrated Pest Management (IPM) [6].

Male *Sitophilus zeamais* produce the aggregation pheromone sitophilure, whose naturally occurring active stereoisomer has been identified as (4*R*,5*S*)-5-hydroxy-4-methylheptan-3-one [7]. In the present study, sitophilure was obtained through a non-stereoselective aldol addition reaction as a racemic mixture of diastereomers, potentially comprising all four stereoisomers.

For field application, three main classes of dispensers are employed: solid matrices, liquid formulations for aerosol, and reservoirs [8]. Over time, rubber septa, sachets, and polyethylene or polyvinyl chloride (PVC) tubes have been used [6, 8]. However, the environmental persistence of these fossil synthetic polymers represents significant ecological damage [9].

In this context, poly(ε-caprolactone) (PCL), a biodegradable and biocompatible semicrystalline aliphatic polyester, is a promising matrix for the sustained release of volatile bioactive compounds. Electrospinning enables the production of continuous polymeric fibers with high specific surface area, high porosity, and tunable morphology, characteristics that are particularly attractive for semiochemical delivery. Electrospun polymeric matrices containing pheromones have demonstrated their potential as controlled-release systems for insect pest management [10, 11]. More recent advances using PCL-containing core-shell fibers have reduced the initial burst release and extended pheromone release for approximately 133 days [12], while biodegradable PHB/PCL electrospun fibers have sustained volatile release for more than 56 days and maintained behavioral activity under laboratory and field conditions [13]. These findings reinforce the potential of electrospun biodegradable matrices as long-lasting semiochemical dispensers. Nevertheless, the use of electrospun PCL matrices for controlled sitophilure release remains scarcely explored, particularly regarding the effect of activated carbon on pheromone retention, thermal behavior, and release kinetics.

Given the above, the objective of this work was to synthesize, electrospin, and characterize PCL mats loaded with the aggregation pheromone sitophilure. The thermal behavior, phase transitions, degradation/release kinetics of the system, structure, morphology, and moisture absorption capacity were evaluated, aiming to consolidate a biodegradable and lower environmental impact alternative for the management of *S. zeamais*.

2. Experimental

2.1 Obtaining the pheromone

Racemic sitophilure (5-hydroxy-4-methylheptan-3-one) was synthesized via a non-stereoselective aldol addition reaction following adapted general synthetic procedures [14, 15]. The synthetic product was considered a racemic mixture of diastereomers, comprising the four possible stereoisomers arising from the two stereogenic centers at C4 and C5. Briefly, a solution of lithium diisopropylamide (LDA) was stirred at -10 °C under a nitrogen atmosphere. A solution of 3-pentanone (5.2 mL, 49.2 mmol) in anhydrous tetrahydrofuran (THF, 10 mL) was added dropwise over 60 min, and the reaction mixture was stirred for an additional 30 min at -10 °C. Subsequently, a solution of propanal (3.8 mL, 53.0 mmol) in anhydrous THF (10 mL) was added dropwise over 60 min, and stirring was continued for another 60 min at -10 °C. The reaction was quenched with 10% aqueous NH_4Cl (50 mL) at -10 °C for 30 min. The organic layer was separated, washed according to established procedures, dried over anhydrous $MgSO_4$, filtered, and concentrated under reduced pressure. The synthesized pheromone was characterized by ^{1}H and ^{13}C NMR, FTIR-ATR, and GC-MS, and its thermal behavior was investigated by TGA and DSC.

2.2 Production of electrospun PCL mats

The polymeric solution was prepared by dissolving 2.0 g of poly(ε-caprolactone) (PCL) in 20 mL of a chloroform/methanol mixture (4:1, v/v), consisting of 16 mL of chloroform and 4 mL of methanol, to obtain a polymer concentration of 10% (w/v). This solution was used as the basis for preparing three formulations: neat PCL, PCL/sitophilure, and PCL/sitophilure/activated carbon.

The neat PCL formulation was prepared using only the polymeric solution, without the addition of sitophilure or activated carbon. For the PCL/sitophilure formulation, 0.2 mL (0.185 g) of sitophilure was added directly to the polymeric solution, without activated carbon, followed by continuous magnetic stirring for 4 h in a closed system to promote homogeneous dispersion. For the PCL/sitophilure/activated carbon formulation, 0.3 g of activated carbon was initially impregnated with 0.2 mL (0.185 g) of sitophilure and maintained at rest for 24 h to allow interaction between the pheromone and the adsorbent. The resulting mixture was subsequently incorporated into the polymeric solution under continuous magnetic stirring for 4 h in a closed system to obtain a homogeneous dispersion.

Electrospinning was performed using an apparatus equipped with a syringe pump and a rotating collector. The processing parameters were an applied voltage of 17 kV, a needle-to-collector distance of 12 cm, a needle internal diameter of 1 mm, a solution flow rate of 1.0 mL h^{-1}, and a collector rotation speed of 30 rpm. The experiments were conducted at an ambient temperature of 25 ± 1 ºC and a relative humidity of 48 ± 5%. The same electrospinning conditions were employed for all three formulations (Fig. 1) [10, 16].

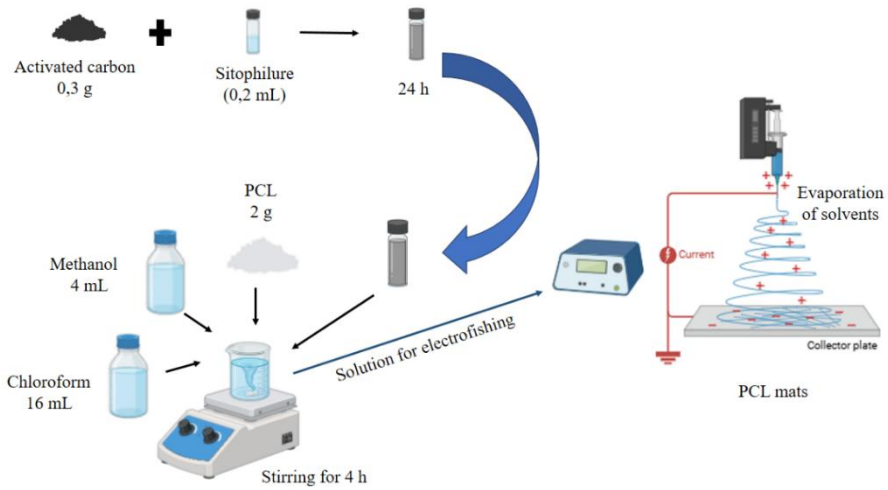

Fig. 1 Diagram of the production process of electrospun mats

2.3 Characterization of the sitophilure pheromone and the electrospun mats

2.3.1 Nuclear magnetic resonance of hydrogen (^{1}H NMR) and carbon-13 (^{13}C NMR) of the sitophilure

^{1}H and ^{13}C nuclear magnetic resonance (NMR) analyses were performed using a Bruker Avance 600 spectrometer operating at 600 MHz for ^{1}H and 150 MHz for ^{13}C (Bruker, Germany). Samples were dissolved in deuterated chloroform ($CDCl_3$) at a concentration of 15 mg mL^{-1}, and measurements were conducted at 300 K. The chemical shift (δ) was expressed in ppm, using tetramethylsilane (TMS) as an internal standard (δ = 0 for ^{1}H and ^{13}C) or the residual hydrogen of $CDCl_3$. Bruker's Top Spin software from Bruker was used for processing the obtained data.

2.3.2 Gas Chromatography-Mass Spectrometry (GC-MS)

Gas chromatography–mass spectrometry (GC–MS) analysis was performed using a Shimadzu GCMS-QP2010 Ultra gas chromatograph coupled to a mass spectrometer (Shimadzu, Japan). A solution of 1 mg mL^{-1} of the synthetic pheromone was prepared in methanol and analyzed under the following conditions: injector temperature = 220 °C; in split mode with a ratio of 1/30; SH-Rxi-5ms column (stationary phase of 5% diphenyl/95% dimethyl polysiloxane with a length of 30 m, an internal diameter of 0.25 mm, and a film thickness of 0.25 µm); column temperature programming = 100 °C for 6 min, followed by heating to 120 °C at a rate of 15 °C min-1, where it remained for an additional 1.67 min. The total analysis time was 9.00 min. The flow rate of Helium gas in the column was 3.0 mL min^{-1} and the interface temperature was 250 °C. Experiments were conducted in full scan mode, where all ions generated in the sample are analyzed (SCAN). LabSolution GC–MS software from Shimadzu was used to process the obtained data.

2.3.3 Scanning Electron Microscope (SEM)

Scanning electron microscopy (SEM) analysis was performed using a TESCAN VEGA3 scanning electron microscope (Tescan, Czech Republic). For the deposition of the dry samples, thin double-sided carbon strips were used on a circular steel sample holder (stub). The metallization of the samples was carried out in a Quorum Q150R ES sputter coater, using a gold target for 2 min, with a current of 10 mA. The SEM operated at 10.0 keV. The field of view was 41 and 104 µm, and the working distance was between 17.32 and 19.30 mm. The scanning of the electrospun mats was carried out at different points of the sample. Vega TC software from Tescan was used for processing the obtained data.

2.3.4 Infrared by Fourier Transform with Attenuated Total Reflectance (FTIR-ATR)

Fourier transform infrared (FTIR) spectra were acquired using a Shimadzu IRAffinity-1 Fourier transform infrared spectrophotometer equipped with an attenuated total reflectance (ATR) accessory (Shimadzu, Japan). The equipment operated in a wavenumber range of 4000 to 650 cm^{-1}, performing 128 scans. The LabSolution IR software from Shimadzu was used for processing the obtained data.

2.3.5 Thermogravimetric Analysis (TGA)

Thermogravimetric analysis (TGA) was performed using a Shimadzu TGA-51 thermogravimetric analyzer (Shimadzu, Japan). The experimental conditions included a heating rate of 10 °C min^{-1}, starting from 30 °C to 900 °C, in a nitrogen atmosphere with a flow rate of 50 mL min^{-1}. The samples, with masses ranging from

10.048 mg to 15.777 mg, were analyzed in platinum crucibles. Tasys software from Shimadzu was used for processing the obtained data.

2.3.6 Differential Scanning Calorimetry (DSC)

Differential scanning calorimetry (DSC) analysis was performed using a Shimadzu DSC-60 differential scanning calorimeter (Shimadzu, Japan). The experimental conditions included a heating rate of 10 °C min^{-1}, starting from 30 °C to 400 °C, in a nitrogen atmosphere with a flow rate of 50 mL min^{-1}. The samples, with masses ranging between 1.100 mg and 3.400 mg, were analyzed in aluminum crucibles. Tasys software from Shimadzu was used for processing the obtained data.

2.3.7 Degree of Swelling (W%)

The hydrophilic properties of the electrospun mats were evaluated by determining their degree of swelling (*W*%) in different aqueous media. Samples with initial dry masses ranging from 3 to 45 mg were individually immersed in 3.0 mL of one of the following media: (i) deionized water at pH 7.0; (ii) 0.10 mol L^{-1} acetate buffer solution at pH 4.0; and (iii) 0.10 mol L^{-1} bicarbonate buffer solution at pH 10.0. The samples were maintained in contact with the respective solutions for 30 min at a controlled ambient temperature of 23 ± 2 °C. After immersion, the mats were removed from the solutions, and excess surface liquid was carefully removed using absorbent paper before weighing. All experiments were performed in triplicate, and the degree of swelling was calculated according to Eq. (1) [17]:

$$W\% = \left(\frac{M_t - M_0}{M_0}\right) 100 \quad (1)$$

where M_t represents the mass of the swollen mat after 30 min of immersion, and M_0 corresponds to the initial dry mass of the same sample before immersion.

2.3.8 Study of the release kinetics of sitophilure incorporated in the mats by isothermal TGA

The temperature-dependent mass-loss behavior of neat sitophilure and electrospun PCL/sitophilure and PCL/sitophilure/activated carbon mats was investigated by isothermal thermogravimetric analysis (TGA). Measurements were performed using a TGA-51 thermobalance (Shimadzu, Japan) under a nitrogen atmosphere at a flow rate of 50 mL min^{-1}. Platinum crucibles were employed, with sample masses ranging from approximately 9.2 to 17.2 mg. Isothermal experiments were conducted at 35, 45, and 55 °C for 12 h (720 min). Thermogravimetric analysis has previously been employed to investigate the evaporation kinetics of volatile organic compounds, providing a gravimetric basis for evaluating temperature-dependent mass-loss behavior [18].

For kinetic analysis, the initial heating and thermal stabilization stages were excluded. Thermal stabilization was identified using a 10 min moving average of the recorded temperature. The beginning of the isothermal fitting interval was defined as the first time at which the moving-average temperature remained within ±0.5 °C of the programmed temperature for at least 20 consecutive minutes. According to this criterion, the fitting intervals began approximately 50 - 53 min after the start of data acquisition, depending on the experiment. The beginning of each selected interval was redefined as $t = 0$, and the corresponding sample mass was taken as M_0. The normalized mass-loss fraction (Q_t) was calculated according to Eq. (2):

$$Q_t = \frac{M_0 - M_t}{m_{s/0}} \quad (2)$$

where M_0 and M_t are the sample masses at the beginning of the selected interval and at time *t*, respectively, and $m_{S/0}$ represents the initial mass of sitophilure present in the analyzed sample. For neat sitophilure, $m_{S/0}$ corresponds to the initial mass of the compound, whereas for the electrospun formulations it represents the initial sitophilure content incorporated into the analyzed mat.

For the kinetic calculations, the initial sitophilure mass in each electrospun mat sample was estimated from the nominal formulation composition, assuming complete incorporation and retention of the pheromone during electrospinning. The nominal sitophilure mass fractions were 8.47 wt% for PCL/sitophilure and 7.44 wt% for PCL/sitophilure/activated carbon. These values were used to normalize the gravimetric mass loss during isothermal TGA.

The normalized gravimetric profiles were evaluated using the zero-order and Korsmeyer–Peppas kinetic models.

The zero-order model was expressed as Eq. (3) [19]:

$$Q_t = k_0 t \quad (3)$$

where k_0 is the zero-order kinetic coefficient (h^{-1}) and t is the elapsed time expressed in hours. This model was included as an empirical reference for evaluating whether the normalized mass-loss response could be approximated by a constant rate over the investigated interval.

The Korsmeyer–Peppas model was expressed according to Eq. (4) [20]:

$$Q_t = K_{KP} t^n \quad (4)$$

where K_{kp} is the empirical kinetic coefficient (h^{-n}) and n is the dimensionless exponent describing the temporal dependence of the normalized mass-loss profile. This power-law relationship was originally developed to describe solute release from polymeric systems and has been widely applied to investigate release behavior in matrices with different geometries and physicochemical characteristics [21].

Although the release exponent n can provide information about transport behavior under the assumptions of the Korsmeyer–Peppas model, its mechanistic interpretation depends on the geometry of the release system and the applicability of the underlying diffusion assumptions [21, 22]. Therefore, in the present study, K_{KP} and n were considered empirical descriptors of the normalized thermogravimetric response rather than definitive indicators of a specific transport mechanism.

The normalized mass-loss profiles were fitted to the zero-order and Korsmeyer–Peppas models by least-squares regression. The zero-order model was fitted by linear regression constrained to pass through the origin, whereas the Korsmeyer–Peppas model was fitted by nonlinear regression. Experimental data were resampled at 1 min intervals for fitting, and time was expressed in hours. The goodness of fit was evaluated using the coefficient of determination (R^2). A sensitivity analysis was also performed by varying the beginning of the fitting interval relative to the identified thermal stabilization time.

2.3.9 In vivo biological assay with olfactometry

To evaluate the behavioral response of unsexed adult *S. zeamais* to the synthetic racemic pheromone sitophilure, dual-choice bioassays were conducted in a Y-tube olfactometer (dimensions: 15.4 cm x 4.4 cm; purified air flow: 800 mL min^{-1}) under red light, in a controlled environment (28 ± 1 °C and 70 ± 2% RH), during the period between 2:00 pm and 9:30 pm. Unsexed insects (1 to 10 days old) were tested individually for 10 min.

Electrospun mats containing sitophilure (20.0 ± 0.1 mg) were placed in one arm of the Y-tube olfactometer, while an electrospun neat PCL mat without sitophilure was placed in the opposite arm as the control. Five repetitions were carried out with 20 insects per treatment, totaling a sample size of (n = 100) individuals per treatment. The position of the olfactometer arms was alternated with each repetition to avoid positional preference. Every two repetitions, the system was sanitized and dried in an oven at 130 °C for 50 min. The olfactory preference data were subjected to the Chi-square (χ^2) goodness-of-fit test at a significance level of 5% [23].

3. Results and Discussion

3.1 Obtaining the pheromone

In the synthesis of the sitophilure pheromone, 4.28 g were obtained, corresponding to a reaction yield of 60.3%. The product was stored in a freezer at 5 ºC. The identity of the pheromone was confirmed by ^{1}H and ^{13}C NMR, GC-MS and FTIR-ATR.

4-methyl-5-hydroxy-3-heptanone (Sitophilure): ^{1}H NMR (600 MHz, $CDCl_3$) δ 0.93-0.98 (m, 3H), 1.03 - 1.06 (m, 3H), 1.11 - 1.13 (m, 3H), 1.35 - 1.58 (m, 3H), 2.34 - 2.66 (m, 3H), 3.54 - 3.82 (m, 1H). ^{13}C NMR (150 MHz, $CDCl_3$) δ 7.5, 7.6, 9.8, 10.4, 14.2, 14.3, 26.9, 27.6, 35.1, 36.0, 49.3, 49.4, 50.6, 50.6, 72.6, 72.7, 75.0, 75.0, 216.7, 216.8. GC–MS (70 eV) m/z (Peak 1): 126 $[M - 18]^+$ (5%), 115 (7%), 86 (20%), 70 (17%), 57 (100%), 41 (9%). GC-MS (70 eV) m/z (Peak 2): 126 $[M - 18]^+$ (7%), 115 (4%), 86 (25%), 70 (11%), 57 (100%), 41 (9%). FTIR-ATR $\tilde{\nu}_{max}$ (cm^{-1}): 3626 - 3194 (O–H), 2970 - 2877 (C–H), 1705 (C=O), 1458 - 1373, 1103 - 1033 (C–O), 972.

3.2 Characterization of electrospun blankets containing the pheromone sitophilure

3.2.1 Scanning Electron Microscope (SEM)

The morphological characterization revealed that the neat PCL mats (Fig. 2A, B) consisted of continuous, slightly wavy fibers with relatively uniform diameters. The incorporation of sitophilure preserved the overall fibrous morphology (Fig. 2C, D), suggesting that its addition did not substantially alter fiber formation. In contrast, the mats containing activated carbon (Fig. 2E, F) exhibited irregular particulate features associated with the fiber surfaces, consistent with the presence of the carbonaceous additive. Previous studies have also reported the incorporation of activated carbon into electrospun PCL-based fibrous structures, highlighting the influence of incorporation strategies on the resulting morphology [24, 25].

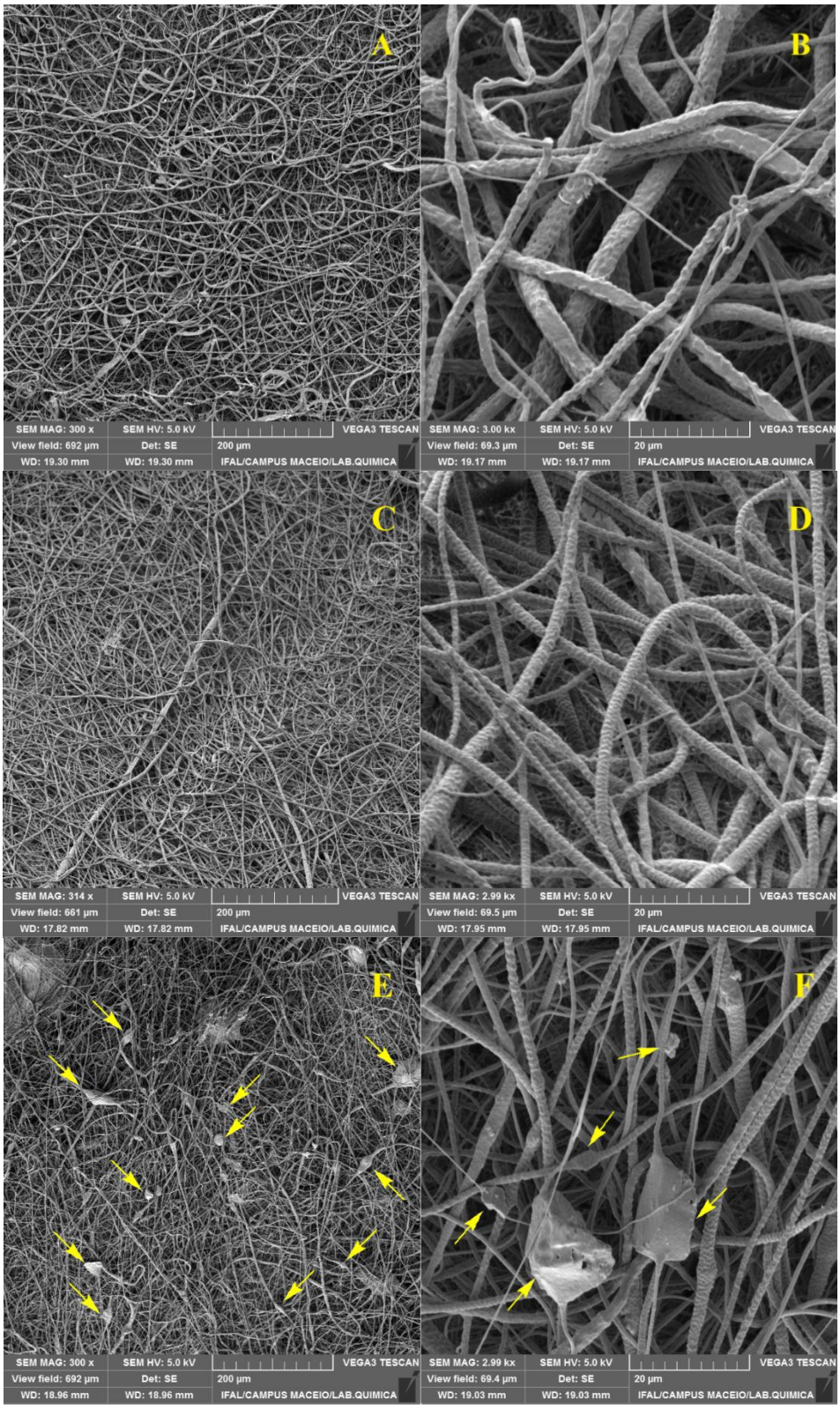

Fig. 2 Scanning electron microscopy (SEM) of PCL-based mats: (A, B) PCL mat; (C, D) PCL/sitophilure mats; and (E, F) PCL/sitophilure/activated carbon mats. The images were acquired with fields of view ranging from 692 µm to 69.3 µm. Yellow arrows indicate the distribution of activated carbon particles

The fiber diameter distributions of the electrospun mats are presented in Fig. 3. The calculated mean fiber diameters were 1380.11 ± 557.41 nm (CV = 40.39%) for neat PCL, 2019.10 ± 581.20 nm (CV = 28.79%) for PCL/sitophilure, and 1085.58 ± 324.31 nm (CV = 29.87%) for PCL/sitophilure/activated carbon. These results demonstrate that the incorporation of sitophilure increased the mean fiber diameter, whereas the addition of

activated carbon resulted in a reduction in fiber diameter. Furthermore, the lower coefficients of variation observed for the sitophilure-containing mats indicate a more uniform fiber diameter distribution compared with neat PCL.

The observed morphological changes may be associated with variations in the physicochemical properties of the electrospinning solutions, including viscosity, electrical conductivity, and charge distribution, which can influence polymer jet stretching and fiber formation [26]. However, these mechanisms were not directly investigated in the present study.

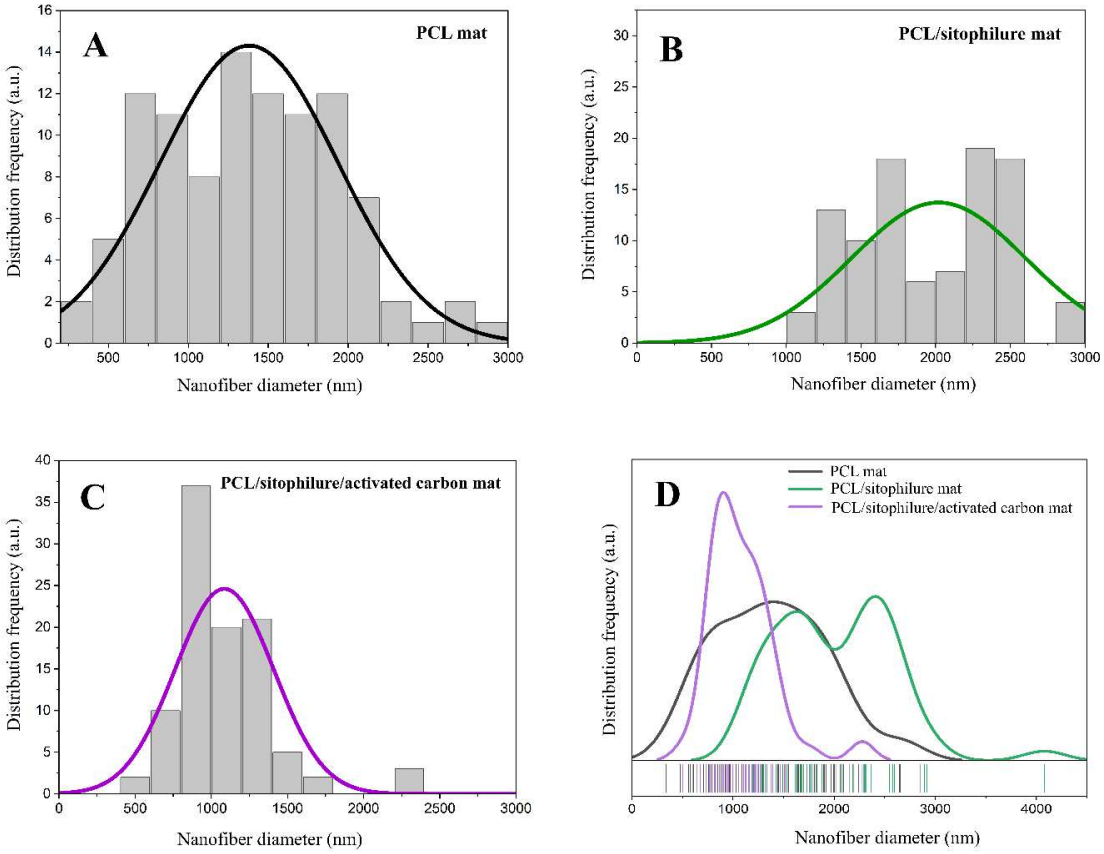

Fig. 3 Fiber diameter distribution histograms and fitted distribution curves for electrospun mats: (A) neat PCL; (B) PCL/sitophilure; (C) PCL/sitophilure/activated carbon; and (D) comparison of the fitted diameter distributions among the formulations

3.2.2 Infrared by Fourier Transform with Attenuated Total Reflectance (FTIR-ATR)

The FTIR-ATR spectrum of sitophilure reveals O-H stretching of alcohol (3626 - 3194 cm^{-1}), aliphatic C-H sp^3 (2970 - 2877 cm^{-1}), and aliphatic C=O of ketone at 1705 cm^{-1}. Angular deformations of methylene CH_2 and methyl CH_3 occur at 1458 - 1373 cm^{-1}, while C-O stretches (1103 -1033 cm^{-1}) indicate secondary alcohol. The narrow signal at 972 cm^{-1} refers to skeletal vibrations and rocking of branched methyls [14, 15] (Fig. 4).

The FTIR-ATR spectrum of commercial activated carbon exhibited relatively weak absorption bands associated with surface functional groups. Absorption in the O–H stretching region (3850–3600 cm^{-1}) may be related to surface hydroxyl groups and adsorbed moisture, whereas the band near 2951 cm^{-1} may be associated with residual aliphatic C–H stretching vibrations. Signals in the 1645–1539 cm^{-1} region may indicate aromatic C=C skeletal vibrations and/or contributions from oxygen-containing surface groups. The band near 1296 cm^{-1} may be tentatively assigned to C–O stretching vibrations associated with oxygen-containing surface functionalities [27, 28]. Additional features at lower wavenumbers may arise from overlapping contributions of different surface groups. These assignments should be considered tentative because the heterogeneous surface chemistry of activated carbon and the overlap of infrared absorption bands limit unambiguous identification. Furthermore, FTIR-ATR alone does not provide quantitative information on pore structure, degree of carbonization, or pyrolysis efficiency [27] (Fig. 4).

The pure PCL mat exhibits a typical profile of aliphatic polyester with C-H sp^3 stretches (2943 - 2866 cm^{-1}) and a strong ester C=O signal at 1722 cm^{-1}. CH_2 deformations (1471 - 1365 cm^{-1}) and the rocking at 732 cm^{-1} indicate long and intact chains. The crystalline C-O and C-C signals (1294 and 1238 cm^{-1}), aligned with the asymmetric C-O-C stretching at 1165 cm^{-1}, confirm the semicrystallinity of the matrix [29] (Fig. 4). The main absorption bands and their respective vibrational assignments are listed in Table 1.

For the PCL/sitophilure mat and PCL/sitophilure/activated carbon mat, the presence of overlapping bands related to pure sitophilure and pure PCL is observed (Fig. 4).

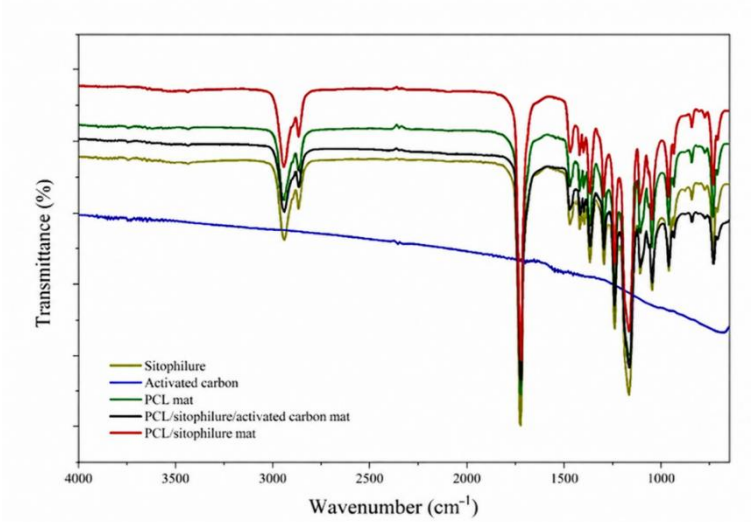

Fig. 4 FTIR-ATR spectra of pure components (sitophilure, activated carbon, and neat electrospun PCL mat) and composite electrospun mats (PCL/sitophilure and PCL/sitophilure/activated carbon), showing characteristic functional groups and vibrational band overlaps

Table 1 Main FTIR-ATR vibrational band assignments, characteristic wavenumbers (cm^{-1}), and spectral profiles for pure components and electrospun PCL mats.

System	Wave number (cm^{-1})	Vibrational Attribution	Intensity and profile of the band
Sitophilure	3626 - 3194	Stretching O-H	Long and defined
	2970 - 2877	Stretching CH_2 and CH_3	Strong and sharp
	1705	Stretching of Aliphatic ketone	Very strong and deep
	1458 - 1373	Angular deformation CH_2 and CH_3	Average
	1103 - 1033	Stretching C-O (secondary alcohol)	Strong
	972	Skeleton vibrations (C-C) and *Rocking* of CH_3	Very strong and narrow
Activated carbon	3850 - 3600	O–H stretching associated with surface hydroxyl groups and/or adsorbed moisture	Weak
	2951	Aliphatic C–H stretching, potentially associated with residual organic surface species	Weak
	1645 - 1539	Aromatic C=C skeletal vibrations and/or contributions from oxygen-containing surface groups	Moderate
	1296	C–O stretching associated with oxygen-containing surface functionalities	Moderate
PCL mat	2945 - 2865	Stretching C-H (sp^3)	Strong and sharp
	1725	Stretching C=O (carbonyl)	Very strong and sharp
	1470 - 1360	Deformation CH_2	Average
	1293	Stretching C-O e C-C (crystal clear)	Strong
	1240 - 1160	Stretching C-O-C (asymmetric)	Strong and wide
	730	Deformation CH_2 (*Rocking*)	Average
PCL/sitophilure mat	3649 - 3435	Stretching O-H (sitophilure)	Weak and wide
	2943 - 2866	Stretching C-H (sp^3)	Strong and sharp
	1722	Stretching C=O (PCL ester and sitophilure ketone)	Very strong and light shoulder
	1471 - 1365	Deformation angular de CH_2 and CH_3	Average

	1240 - 1165	Stretching C-O and C-C (crystalline phase of PCL)	Strong
	1045	Stretching C-O (PCL + Sitophilure)	Strong and accented
	732	Deformation of CH_2 (*Rocking*) from the matrix of PCL	Average
PCL/sitophilure/activated carbon mat	3450 - 3350	Stretching O-H (Sitophilure)	Weak and wide
	2945 - 2865	Stretching C-H (sp^3)	Strong and sharp
	1725	Stretching C=O (PCL ester and Sitophilure ketone)	Very strong and wide
	1580 - 1600	Stretching C=C (activated carbon)	Subtle and overlaid
	1470 - 1360	Deformation CH_2 and CH_3	Average
	1293	Stretching C-O and C-C (crystal clear)	Strong
	1240 - 1050	Stretching C-O (PCL + Sitophilure)	Strong and accented
	730	Deformation CH_2 (*Rocking*)	Average

Note: The frequencies are expressed in wavenumbers (cm^{-1}). Stretching: vibration along the axis of the chemical bond; Angular deformation: vibration that alters the angle between bonds; sp^3: hybridization of saturated carbons; The term "shoulder" refers to a secondary band that appears partially overlapping a main band. All values were estimated based on overlaps or limitations in the software marking.

3.2.3 Thermogravimetric Analysis (TGA)

Thermogravimetric analysis (TGA) was performed to evaluate the thermal behavior, mass-loss stages, and residual mass of pure sitophilure, activated carbon, neat electrospun PCL mats, and binary and ternary composite mats (Fig. 5). The thermogravimetric profiles revealed distinct thermal responses associated with the physicochemical characteristics of the individual components and changes resulting from their incorporation into the electrospun polymeric matrix. Previous studies have demonstrated that the incorporation of additional components into PCL-based formulations can modify their thermal degradation behavior, depending on the composition and interactions between the constituents [30, 31]. The corresponding mass-loss percentages and characteristic temperatures are summarized in Table 2.

Pure sitophilure exhibited a thermal profile characterized by pronounced mass loss below 200 °C, consistent with the volatile nature of this low-molecular-weight organic compound. Two main mass-loss stages were identified. The first occurred between an onset temperature (T_{onset}) of 133.03 °C and an endset temperature (T_{endset}) of 158.78 °C, with a maximum mass-loss rate (T_p) at 158.99 °C and a mass loss of 70.09%. This event is predominantly associated with the volatilization of sitophilure, although contributions from other volatile constituents cannot be excluded. The second stage occurred between 169.36 and 181.56 °C, with T_p at 173.70 °C and an additional mass loss of 29.64%, potentially involving the volatilization or thermal decomposition of residual compounds and synthesis byproducts. The low final residue (0.269%) indicates that the sample was almost completely volatilized or decomposed under the experimental conditions. These results demonstrate the pronounced thermal sensitivity of pure sitophilure and provide a reference for evaluating its behavior following incorporation into the polymeric formulations.

Activated carbon exhibited a markedly different thermogravimetric profile, characterized by an initial mass-loss stage of 11.09% between 59.07 and 81.57 °C, with T_p at 65.99 °C. This event can be attributed primarily to the desorption of physically adsorbed moisture and volatile species retained within the porous carbonaceous structure. Following this initial stage, the material exhibited comparatively limited mass loss until approximately 591.26 °C, when a second major thermal event was detected. This stage extended from 591.26 to 660.76 °C, with T_p at 646.00 °C and a mass loss of 80.47%, indicating extensive thermal transformations of the carbonaceous material under the experimental conditions. The final residue was 8.439%. The substantial difference between the thermal profiles of sitophilure and activated carbon highlights their distinct physicochemical characteristics, particularly the greater resistance of the carbonaceous material to mass loss at intermediate temperatures. Previous studies have also investigated the thermal behavior and physicochemical properties of activated carbon materials [27, 32].

The neat electrospun PCL mat exhibited three mass-loss stages. The first was a minor event of 0.44%, occurring between 117.69 and 130.94 °C, with T_p at 124.00 °C, which may be associated with the evaporation of residual solvent or other low-molecular-weight volatile compounds remaining after electrospinning. The low magnitude of this event indicates that the polymeric matrix underwent negligible mass loss within this temperature interval. The principal decomposition stage occurred between T_{onset} = 399.60 °C and T_{endset} = 424.73 °C, with T_p at 417.17 °C, corresponding to a mass loss of 86.21%. This event is attributed to the thermal degradation of the aliphatic polyester chains, consistent with the characteristic thermal decomposition behavior of PCL reported in

previous studies [30, 31]. A subsequent mass-loss stage of 13.03% was observed between 452.63 and 484.40 °C, with T_p at 468.50 °C, indicating further decomposition of the remaining polymeric material. This process may involve secondary degradation and depolymerization reactions, potentially including the formation of ε-caprolactone, as discussed in the literature on PCL thermal degradation [30]. However, identification of the evolved products would require complementary analytical techniques. The final residue of 0.320% indicates almost complete decomposition of the organic polymeric matrix.

The binary PCL/sitophilure mat exhibited an initial mass-loss stage of 3.04%, occurring between T_{onset} = 77.38 °C and T_{endset} = 84.16 °C, with T_p at 80.00 °C. This event may be associated with the removal of volatile constituents, potentially including sitophilure. Notably, the initial mass-loss peak occurred at a substantially lower temperature than the main volatilization-related event of pure sitophilure (T_p = 158.99 °C). This difference suggests that the thermal behavior of the volatile constituents is modified following incorporation into the electrospun PCL matrix. The main decomposition event occurred between 390.82 and 425.94 °C, with T_p at 415.44 °C and a mass loss of 85.44%, corresponding predominantly to degradation of the PCL matrix. Compared with neat PCL (T_p = 417.17 °C), the difference of 1.73 °C indicates that sitophilure incorporation produced only a minor change in the temperature of the principal polymer degradation peak. A third stage, representing 10.58% mass loss, was observed between approximately 450.00 and 520.00 °C, with T_p at 479.90 °C, and may be associated with further decomposition of the remaining polymeric material. The final residue was 0.938%, slightly higher than that of the neat PCL mat.

The ternary PCL/sitophilure/activated carbon mat exhibited three main mass-loss stages, with a thermogravimetric profile distinct from that of the binary formulation. The first event occurred between T_{onset} = 101.37 °C and T_{endset} = 177.19 °C, with T_p at 136.61 °C and a mass loss of 4.17%. This event may involve the removal of volatile constituents, including sitophilure, residual solvent, and adsorbed moisture. Compared with the binary PCL/sitophilure mat, the onset temperature increased from 77.38 to 101.37 °C, while the temperature of the maximum mass-loss rate increased from 80.00 to 136.61 °C, corresponding to shifts of 23.99 and 56.61 °C, respectively. These changes suggest that the incorporation of activated carbon modifies the thermal removal of volatile compounds from the electrospun matrix. Considering the porous nature and adsorption capacity of activated carbon [27, 32], this behavior is compatible with a possible contribution of adsorption-related interactions that influence the retention and subsequent removal of volatile constituents. Nevertheless, the mass-loss event cannot be assigned exclusively to sitophilure, and the observed temperature shifts do not independently demonstrate controlled pheromone release.

The principal mass-loss stage of the ternary formulation occurred between T_{onset} = 375.02 °C and T_{endset} = 414.95 °C, with T_p at 389.13 °C and a mass loss of 71.99%. This event is predominantly associated with decomposition of the PCL matrix, although the presence of activated carbon may modify the degradation behavior and the relative contributions of overlapping thermal processes. Previous studies have demonstrated that the incorporation of additional components into PCL-based formulations can influence their thermal degradation behavior [30, 31]. Compared with the binary formulation, the main decomposition peak shifted from 415.44 to 389.13 °C, representing a decrease of 26.31 °C. A similar reduction was observed in the onset temperature, from 390.82 to 375.02 °C. These results indicate that the incorporation of activated carbon did not increase the thermal resistance of the polymeric matrix to its principal decomposition process. Instead, the carbonaceous component altered the overall thermal response of the composite, resulting in an earlier occurrence of the dominant mass-loss stage. The final mass-loss stage, corresponding to 22.81%, occurred between 491.06 and 547.24 °C, with T_p at 511.13 °C. This event may involve secondary decomposition of the remaining polymeric constituents and thermal transformations of carbonaceous residues. The final residue was 1.022%, slightly higher than those observed for neat PCL and the binary formulation.

A comparative evaluation of the thermogravimetric profiles reveals two important effects associated with activated carbon incorporation. First, the displacement of the initial mass-loss event toward higher temperatures suggests changes in the retention or thermal removal of volatile constituents within the ternary composite. This finding is particularly relevant to the development of polymeric pheromone-delivery systems, since the release behavior of volatile compounds is an important consideration in the design of controlled-release devices [6, 11]. Second, the decrease in the principal PCL decomposition temperature demonstrates that the thermal behavior of the polymeric matrix is also affected by activated carbon incorporation. Therefore, the observed changes should be interpreted as modifications of the composite thermal response rather than as evidence of an overall improvement in thermal stability.

Overall, the TGA results demonstrate that pure sitophilure undergoes substantial mass loss below 200 °C, whereas neat PCL exhibits its main decomposition stage at approximately 417 °C. Incorporation of sitophilure into the electrospun matrix produced only a minor change in the principal PCL degradation peak. In contrast, activated carbon incorporation shifted the initial mass-loss event of the binary formulation toward higher temperatures while reducing the temperature of the main polymer decomposition peak. These findings suggest that activated carbon influences both the thermal removal of volatile constituents and the degradation behavior of the polymeric matrix. However, confirmation of its specific contribution to sitophilure retention and controlled release

requires complementary release measurements. Accordingly, the TGA results provide a basis for interpreting the thermal characteristics of the developed electrospun formulations and support their subsequent evaluation as potential pheromone-delivery systems.

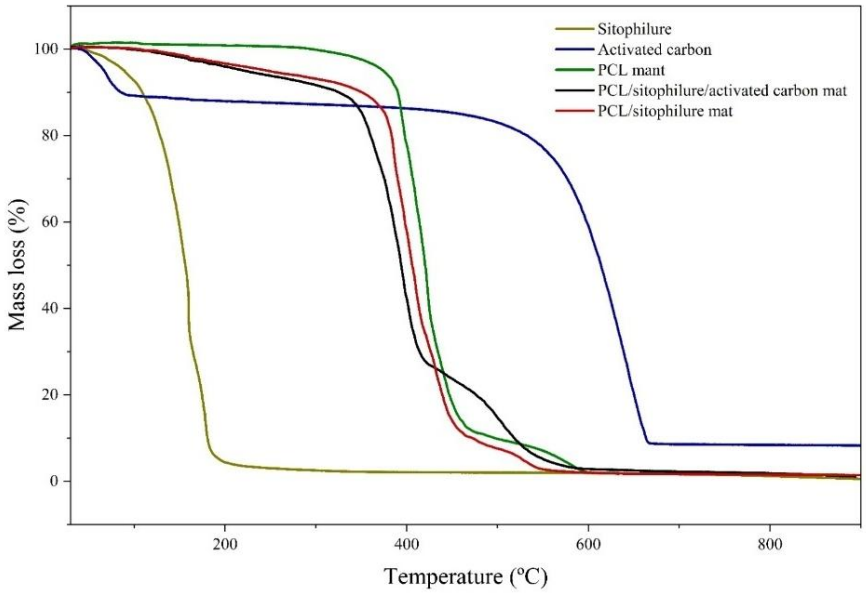

Fig. 5 Thermogravimetric analysis (TGA) thermal degradation profiles and volatilization behavior of pure sitophilure, activated carbon, neat electrospun PCL mat, and composite PCL mats loaded with sitophilure (PCL/sitophilure) and sitophilure/activated carbon (PCL/sitophilure/activated carbon)

Table 2 Degradation temperatures and mass loss percentages obtained by TGA of the pheromone and the electrospun mats.

System	Mass (mg)	Main stages of mass loss (TGA)	Residue (%)
Sitophilure	11.139	70.09 %; T_{onset} = 133.03 ºC; T_{endset} = 158.78 ºC; T_p = 158.99 ºC: Event potentially associated with volatile components, including sitophilure. 29.64 %; T_{onset} = 169.36 ºC; T_{endset} = 181.56 ºC; T_p = 173.70 ºC: Volatilization or decomposition of by-products.	0.269
Activated carbon	10.048	11.09%; T_{onset} = 59.07 ºC; T_{endset} = 81.57 ºC; T_p = 65.99 ºC: Desorption of moisture and volatiles. 80.47%; T_{onset} = 591.26 ºC; T_{endset} = 660.76 ºC; T_p = 646.00 ºC: Thermal transformations of the carbonaceous material.	8.439
PCL mat	11.260	0.44%; T_{onset} = 117.69 ºC; T_{endset} = 130.94 ºC; T_p = 124.00 ºC: Volatilization of residual compounds. 86.21%; T_{onset} = 399.60 ºC; T_{endset} = 424.73 ºC; T_p = 417.17 ºC: Thermal decomposition (aliphatic polyesters). 13.03%; T_{onset} = 452.63 ºC; T_{endset} = 484.40 ºC; T_p = 468.50 ºC: Secondary thermal degradation of residual polymeric material.	0.320
PCL/sitophilure mat	15.777	3.04%; T_{onset} = 77.38 ºC; T_{endset} = 84.16 ºC; T_p = 80.00 ºC: Potentially associated with volatile components, including sitophilure. 85.44%; T_{onset} = 390.82 ºC; T_{endset} = 425.94 ºC; T_p = 415.44 ºC: Decomposition of PCL. 10.58%; T_{onset} = 450.00 ºC; T_{endset} = 520.00 ºC; T_p = 479.90 ºC: Final depolymerization.	0.938
PCL/sitophilure/activated carbon mat	13.098	4.17%; T_{onset} = 101.37 ºC; T_{endset} = 177.19 ºC; T_p = 136.61 ºC: Potentially associated with volatile components, including sitophilure. 71.99%; T_{onset} = 375.02 ºC; T_{endset} = 414.95 ºC; T_p = 389.13 ºC: Decomposition of PCL.	1.022

	22.81%; T_{onset} = 491.06 ºC; T_{endset} = 547.24 ºC; T_p = 511.13 ºC: Secondary degradation and thermal transformations of residual material.

Note: Tonset: onset temperature of the mass-loss stage; Tendset: end temperature of the mass-loss stage; Tp: temperature corresponding to the maximum mass-loss rate (DTG peak). Some values were estimated due to overlapping thermal events or limitations in the software peak identification.

3.2.4 Differential Scanning Calorimetry (DSC)

Differential scanning calorimetry (DSC) was employed to investigate the thermal transitions of pure sitophilure, activated carbon, neat electrospun poly(ε-caprolactone) (PCL) mats, and binary and ternary composite mats (Fig. 6). The thermograms exhibited endothermic events whose peak temperatures and enthalpy changes varied according to the composition of each system. DSC provides information on the melting behavior of semicrystalline polymers and the energetic changes associated with thermal transformations. Previous studies have demonstrated that the thermal behavior of PCL-based materials is influenced by polymer composition, crystalline organization, intermolecular interactions, and the incorporation of additional compounds or fillers [33-39]. The characteristic calorimetric parameters obtained for the investigated materials are summarized in Table 3.

Pure sitophilure exhibited three endothermic events at peak temperatures (T_p) of 153.16, 186.13, and 205.85 °C, with corresponding enthalpy changes (ΔH) of -19.75, -94.56, and -34.28 J g^{-1}, respectively. The first event occurred within the temperature interval associated with the main mass-loss stage identified by TGA, which exhibited a maximum mass-loss rate at 158.99 °C and accounted for 70.09% of the initial sample mass (Fig. 5). This correspondence supports the contribution of volatilization to the observed calorimetric response. The second endothermic peak, at 186.13 °C, exhibited the highest enthalpy magnitude, suggesting a substantial heat-absorbing process involving the remaining volatile constituents. The third event, at 205.85 °C, may be associated with additional thermal transformations of residual compounds. However, the TGA results indicated that almost complete mass loss occurred below approximately 200 °C, with a final residue of only 0.269%.

Activated carbon exhibited two endothermic events, centered at 102.59 °C (ΔH = -231.46 J g^{-1}) and 244.29 °C (ΔH = -107.86 J g^{-1}). The first event is consistent with the desorption of physically adsorbed moisture and volatile compounds retained within the porous carbonaceous structure. This interpretation is supported by the initial mass-loss stage identified by TGA, which accounted for 11.09% of the sample mass and exhibited a maximum mass-loss rate at 65.99 °C. Although the peak temperatures obtained by the two techniques differ, both events occur within a relatively low-temperature region associated with the removal of volatile species. The second DSC event extended over a broad temperature interval, from 176.78 to 344.86 °C, and may involve the desorption of more strongly retained compounds or thermal transformations of surface-associated species. Notably, the TGA profile indicated that the principal mass-loss stage of activated carbon occurred at substantially higher temperatures, with T_p = 646.00 °C. Thus, the endothermic event observed at 244.29 °C should not be directly attributed to the main degradation of the carbonaceous structure. These results highlight the distinct thermal response of activated carbon and the importance of considering both calorimetric and gravimetric evidence when interpreting its behavior.

The DSC curve of the neat electrospun PCL mat exhibited a well-defined endothermic peak at T_p = 63.31 °C (ΔH = -61.99 J g^{-1}), corresponding to the melting of crystalline domains of poly(ε-caprolactone). This behavior is consistent with the semicrystalline nature of PCL and agrees with previous studies reporting melting transitions in the range of approximately 55 - 65 °C. Mohamed et al. [31] reported a melting temperature of 56.6 °C for neat PCL, while Salom et al. [37] confirmed the characteristic melting behavior associated with its crystalline phase. Similarly, Tabia et al. [35] investigated the thermal behavior and crystallinity of electrospun PCL-based fibers using DSC. The melting transition observed at 63.31 °C is also consistent with the TGA results, which showed that the neat PCL mat underwent negligible mass loss at temperatures close to its melting point. A minor mass-loss event of 0.44% was detected between 117.69 and 130.94 °C, whereas the principal decomposition stage began at 399.60 °C, with a maximum mass-loss rate at 417.17 °C. These findings indicate that the endothermic peak observed by DSC corresponds to the physical melting of crystalline PCL domains rather than polymer degradation, demonstrating the distinction between the melting transition and the onset of substantial thermal decomposition.

For the binary PCL/sitophilure mat, the DSC curve exhibited a characteristic endothermic melting peak at T_p = 59.04 °C (ΔH = -24.17 J g^{-1}), representing a decrease of 4.27 °C compared with neat PCL (T_p = 63.31 °C). This reduction demonstrates that the incorporation of sitophilure altered the melting behavior of the polymeric matrix while preserving the characteristic melting transition of semicrystalline PCL. Previous studies have demonstrated that the incorporation of additional compounds into PCL-based systems affects their thermal behavior and crystalline organization [35, 38, 39]. The apparent melting enthalpy decreased from -61.99 J g^{-1} for neat PCL to -24.17 J g^{-1} for the binary formulation, confirming a substantial change in the calorimetric response associated with the melting transition. This difference reflects the combined influence of formulation composition and the thermal organization of the electrospun polymeric matrix.

At higher temperatures, the DSC curve of the binary PCL/sitophilure mat exhibited additional endothermic features at T_p = 255.73 °C (ΔH = −0.61 J g^{-1}) and 347.21 °C (ΔH = −19.98 J g^{-1}). These features demonstrate that the binary formulation exhibits calorimetric responses beyond the characteristic melting region of PCL. The event at 255.73 °C presented a relatively small enthalpy magnitude, whereas the feature at 347.21 °C showed a more pronounced endothermic contribution. The TGA results identified the principal decomposition peak of the binary formulation at T_p = 415.44 °C, close to the corresponding value for neat PCL (T_p = 417.17 °C), representing a difference of only 1.73 °C. This agreement demonstrates that sitophilure incorporation preserved the temperature of maximum polymer mass loss despite the changes observed in the DSC curve. Together, the DSC and TGA results establish that sitophilure incorporation modifies the calorimetric behavior of the electrospun matrix while maintaining the characteristic melting transition and the principal thermal degradation temperature of PCL.

The ternary PCL/sitophilure/activated carbon mat exhibited a characteristic PCL melting peak at T_p = 58.85 °C (ΔH = -22.73 J g^{-1}). Compared with neat PCL and the binary formulation, the melting temperature decreased by 4.46 and 0.19 °C, respectively. These results indicate that the incorporation of sitophilure and activated carbon was associated with changes in the melting behavior of the PCL-based mats, while preserving the characteristic endothermic transition of the semicrystalline polymer. Tabia et al. [35] demonstrated that the incorporation of bioactive glass nanoparticles can influence the thermal behavior and crystallinity of electrospun PCL fibers, while Simão et al. [39] investigated the effects of cellulose nanocrystals on the crystallization behavior of PCL-containing composites. Although these systems differ from the present formulation, they provide evidence that incorporated components can modify the thermal organization of PCL-based materials. The apparent melting enthalpy of the ternary formulation was -22.73 J g^{-1}, compared with -24.17 J g^{-1} for the binary mat and -61.99 J g^{-1} for neat PCL. Nevertheless, these differences should not be interpreted as direct evidence of changes in crystallinity without accounting for the polymer mass fraction and the specific thermal history of each formulation.

The ternary formulation also exhibited two additional endothermic events at T_p = 234.92 °C (ΔH = -0.62 J g^{-1}) and 348.78 °C (ΔH = -3.02 J g^{-1}). Compared with the binary mat, the intermediate peak shifted from 255.73 to 234.92 °C, corresponding to a decrease of 20.81 °C, whereas the high-temperature peak remained relatively unchanged, increasing from 347.21 to 348.78 °C. However, the enthalpy magnitude associated with the latter event decreased considerably, from 19.98 to 3.02 J g^{-1}. These differences indicate that activated carbon modifies the overall calorimetric response of the composite system, potentially through changes in the relative contributions of the constituent materials and adsorption-related interactions. Nevertheless, the reduced enthalpy magnitude cannot be directly interpreted as evidence of increased thermal stability or enhanced sitophilure retention.

The comparison between DSC and TGA provides additional information regarding the influence of activated carbon on the thermal behavior of the composite mats. The first mass-loss peak of the binary PCL/sitophilure mat occurred at 80.00 °C, whereas the corresponding event in the ternary formulation was observed at 136.61 °C, representing an increase of 56.61 °C. Similarly, the onset temperature of this stage increased from 77.38 to 101.37 °C. These results indicate that activated carbon incorporation modified the temperature range associated with the removal of volatile constituents. Considering the porous structure of activated carbon, this behavior is compatible with a possible contribution of adsorption-related interactions that affect the retention and subsequent removal of volatile compounds. However, the mass-loss events may also include contributions from residual solvent and moisture, preventing an unequivocal assignment to sitophilure release. Conversely, the main degradation peak identified by TGA shifted from 415.44 °C in the binary mat to 389.13 °C in the ternary formulation, indicating that activated carbon incorporation anticipated the principal decomposition process of the PCL-containing matrix. Therefore, the combined thermal results suggest that activated carbon modifies the removal of volatile constituents and the degradation behavior of the composite without necessarily improving its overall thermal stability.

Overall, DSC analysis demonstrated that the incorporation of sitophilure and activated carbon was associated with a decrease in the characteristic melting temperature of PCL, from 63.31 °C for the neat electrospun mat to 59.04 and 58.85 °C for the binary and ternary formulations, respectively. Despite these shifts, the characteristic melting transition of semicrystalline PCL was preserved in both composite mats. The differences in apparent melting enthalpy suggest changes in the calorimetric response of the formulations, although their interpretation in terms of polymer crystallinity requires consideration of the PCL mass fraction. In conjunction with TGA, the results indicate that activated carbon incorporation shifted the initial mass-loss event toward higher temperatures while promoting an earlier occurrence of the main polymer degradation stage. These findings demonstrate that the incorporation of additional components modifies the thermal behavior of the electrospun formulations, without independently establishing the mechanism of sitophilure retention or controlled release. The release-related performance of the developed formulations was therefore investigated separately through isothermal thermogravimetric measurements at 35, 45, and 55 °C.

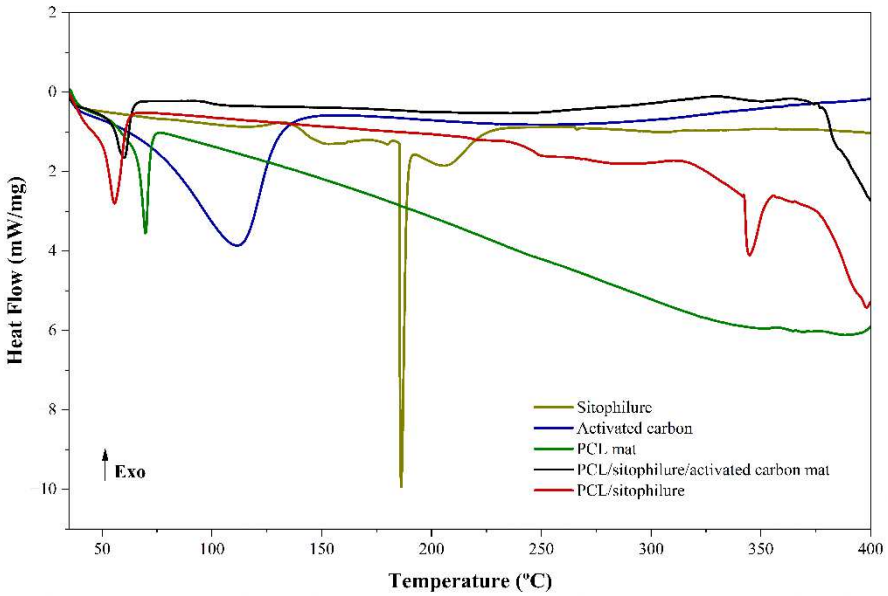

Fig. 6 Differential scanning calorimetry (DSC) curves showing thermal transitions of pure sitophilure, activated carbon, neat electrospun PCL mat, and composite PCL/sitophilure and PCL/sitophilure/activated carbon mats

Table 3 Calorimetric parameters, transition temperatures (T_{onset}, T_{endset}, T_p), and enthalpy changes (ΔH) obtained by DSC for sitophilure, activated carbon, neat PCL, and composite electrospun mats.

System	Mass (mg)	Main thermal events (DSC)
Sitophilure	1.100	T_p = 153.16 °C; ΔH = -19.75 J g^{-1}: Endothermic event associated with the initial volatilization region. T_p = 186.13 °C; ΔH = -94.56 J g^{-1}: Main high-enthalpy endothermic event. T_p = 205.85 °C; ΔH = -34.28 J g^{-1}: Additional endothermic thermal event.
Activated carbon	3.400	T_p = 102.59 °C; ΔH = -231.46 J g^{-1}: Desorption of moisture and volatile compounds. T_p = 244.29 °C; ΔH = -107.86 J g^{-1}: Endothermic event potentially involving strongly adsorbed species or surface-associated compounds.
PCL mat	1.500	T_p = 63.31 °C; ΔH = -61.99 J g^{-1}: Melting of crystalline PCL domains.
PCL/sitophilure mat	3.300	T_p = 59.04 °C; ΔH = -24.17 J g^{-1}: Melting of crystalline PCL domains. T_p = 255.73 °C; ΔH = -0.61 J g^{-1}: Intermediate endothermic event. T_p = 347.21 °C; ΔH = -19.98 J g^{-1}: High-temperature endothermic transformation.
PCL/sitophilure/activated carbon mat	3.200	T_p = 58.85 °C; ΔH = -22.73 J g^{-1}: Melting of crystalline PCL domains. T_p = 234.92 °C; ΔH = -0.62 J g^{-1}: Intermediate endothermic event. T_p = 348.78 °C; ΔH = -3.02 J g^{-1}: High-temperature endothermic transformation.

Note: T_{onset}: initial temperature of the thermal event; T_{endset}: final temperature of the event; T_p: peak temperature; ΔH: enthalpy change (heat involved in the transition). All values were estimated due to overlaps or limitations in the software marking.

3.2.5 Degree of Swelling (W%)

The swelling behavior of the electrospun mats was strongly influenced by both the incorporation of sitophilure and the composition of the immersion medium (Table 4). The pristine PCL mat exhibited relatively low swelling, with W% values of 19.2 ± 1.4% in deionized water, 8.3 ± 0.5% in acetate buffer (pH 4.0), and 5.7 ±

1.5% in bicarbonate buffer (pH 10.0). These results are consistent with the predominantly hydrophobic nature of PCL, which limits water uptake by the polymer matrix.

The incorporation of sitophilure markedly increased the swelling capacity of the PCL mat. The PCL/sitophilure system exhibited mean W% values of 319.9 ± 56.5% in deionized water, 422.1 ± 162.5% at pH 4.0, and 264.9 ± 142.2% at pH 10.0. Sitophilure contains hydroxyl and carbonyl functional groups that may favor polar interactions with the aqueous medium. However, the substantial increase in swelling may also be associated with changes in fiber morphology, porosity, and polymer-chain packing induced by incorporation of the active compound.

The addition of activated carbon reduced the swelling relative to the PCL/sitophilure mat, particularly in deionized water, for which the PCL/sitophilure/activated carbon mat exhibited a W% of 112.0 ± 31.2%. In acetate buffer at pH 4.0 and bicarbonate buffer at pH 10.0, mean values of 286.3 ± 75.5% and 246.1 ± 123.5%, respectively, were obtained. This reduction may be associated with restriction of the effective mobility and free volume of the polymer-rich phase and with interactions between sitophilure and the porous activated carbon. These interpretations should, however, be considered mechanistic hypotheses rather than direct measurements of polymer-chain mobility .

The relatively high standard deviations observed for some sitophilure-containing systems, particularly at pH 4.0 and pH 10.0, indicate considerable variability among replicates. This behavior may reflect heterogeneity in the electrospun mats, including local differences in fiber packing, porosity, active-compound distribution, and liquid penetration.

Table 4. Degree of swelling (W%) of biodegradable electrospun PCL-based mats in different immersion media.

System	deionized water *W%*	Acetate buffer pH 4.0 *W%*	Bicarbonate buffer pH 10.0 *W%*
PCL mat	19.2 ± 1.4	8.3 ± 0.5	5.7 ± 1.5
PCL/sitophilure mat	319.9 ± 56.5	422.1 ± 162.5	264.9 ± 142.2
PCL/sitophilure/activated carbon mat	112.0 ± 31.2	286.3 ± 75.5	246.1 ± 123.5

Note: Values are expressed as mean ± standard deviation (SD), n = 3. *W%*: degree of swelling.

3.2.6 Isothermal thermogravimetric analysis and apparent release kinetics

The isothermal thermogravimetric curves of neat sitophilure, PCL/sitophilure mats, and PCL/sitophilure/activated carbon mats at 35, 45, and 55 °C are presented in Fig. 7. The experimental profiles reveal distinct mass-retention behaviors depending on temperature and formulation composition. Neat sitophilure exhibited the most pronounced mass reduction, particularly at 55 °C, whereas the electrospun formulations maintained a substantially higher percentage of their initial total mass throughout the investigated period. This difference is consistent with the presence of the PCL-based matrix, which constitutes most of the mass of the electrospun samples.

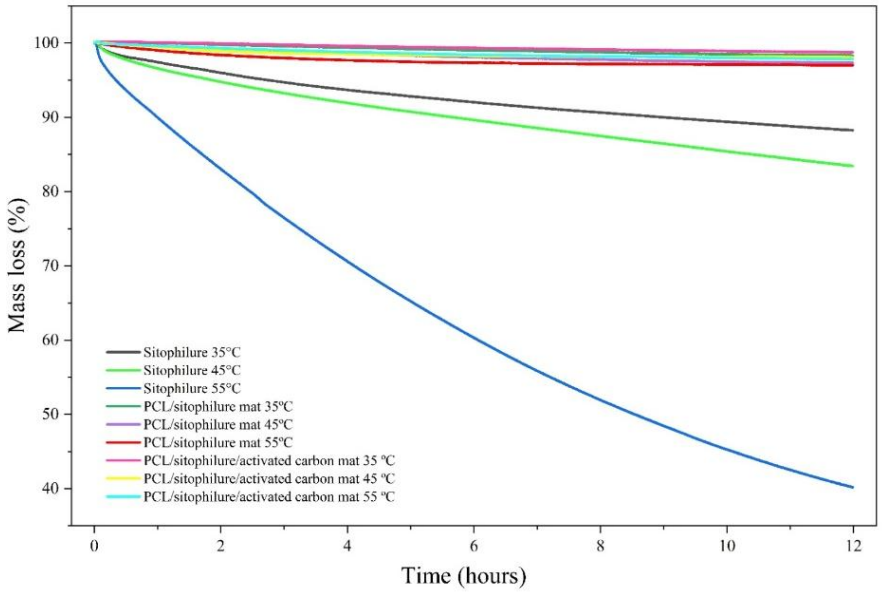

Fig. 7 Thermogravimetric mass-loss profiles of neat sitophilure, PCL/sitophilure, and PCL/sitophilure/activated carbon recorded at programmed temperatures of 35, 45, and 55 °C over the complete 720 min acquisition period, including the initial heating and thermal stabilization stages. Kinetic fitting was performed exclusively on the

thermally stabilized portions of the experimental profiles, with the beginning of each selected interval redefined as $t = 0$.

For neat sitophilure, the remaining mass decreased progressively with increasing temperature, with the greatest reduction observed at 55 °C. In contrast, the PCL/sitophilure and PCL/sitophilure/activated carbon formulations exhibited comparatively small changes in total sample mass over the 12 h period. Although the incorporation of activated carbon modified the thermogravimetric profiles, the differences among the polymeric formulations were relatively small on the total-mass scale shown in Fig. 7. Therefore, the apparent influence of activated carbon should be assessed using the normalized gravimetric data and kinetic parameters reported in Table 5, rather than inferred solely from the visual separation of the curves.

The normalized mass-loss profiles were fitted to the zero-order and Korsmeyer–Peppas kinetic models using the thermally stabilized portions of the experimental curves. The recalculated parameters are presented in Table 5. The Korsmeyer–Peppas model provided a satisfactory empirical description of the nine experimental profiles, with R^2 values ranging from 0.9393 to 0.9999. The fitted exponent n ranged from 0.7273 to 0.8301 for neat sitophilure, from 0.4123 to 0.5548 for PCL/sitophilure, and from 0.3585 to 0.7233 for PCL/sitophilure/activated carbon. These variations indicate formulation- and temperature-dependent differences in the temporal evolution of normalized mass loss. However, the exponent values should not be interpreted as definitive evidence of a specific diffusion mechanism, because the measurements reflect apparent gravimetric behavior rather than compound-specific pheromone release [20, 21].

Table 5 Empirical kinetic parameters obtained by fitting the zero-order and Korsmeyer–Peppas models to normalized isothermal thermogravimetric mass-loss profiles of neat sitophilure, PCL/sitophilure, and PCL/sitophilure/activated carbon at 35, 45, and 55 °C, using data acquired after thermal stabilization

System	Temperature (°C)	k_0 (h^{-1})	R^2 (Zero-order)	K_{KP} (h^{-n})	n	R^2 (Korsmeyer–Peppas)
Pure sitophilure	35	0.01478	0.9438	0.02593	0.7273	0.9999
	45	0.02242	0.9824	0.03186	0.8301	0.9999
	55	0.05718	0.9489	0.09619	0.7479	0.9953
PCL/sitophilure mat	35	0.02799	0.7367	0.06969	0.5548	0.9753
	45	0.03316	0.5530	0.09620	0.4806	0.9611
	55	0.03009	0.2763	0.10031	0.4123	0.9489
PCL/sitophilure/activated carbon mat	35	0.02825	0.9398	0.04992	0.7233	0.9983
	45	0.02449	−0.0707	0.09077	0.3585	0.9393
	55	0.03087	0.5263	0.09151	0.4687	0.9759

Note: k_0 is the zero-order kinetic coefficient; K_{KP} is the Korsmeyer–Peppas kinetic coefficient; n is the dimensionless empirical exponent; and R^2 is the coefficient of determination. The fitting interval was selected using a temperature-stabilization criterion based on a 10 min moving average within ±0.5 °C of the programmed temperature for at least 20 consecutive minutes. The normalized mass loss was calculated using the nominal initial sitophilure content, assuming complete incorporation and retention during electrospinning. Since unloaded-matrix controls were unavailable, the fitted parameters represent apparent release-related gravimetric behavior rather than compound-specific sitophilure release.

Overall, the isothermal thermogravimetric results demonstrate that incorporation into electrospun PCL matrices modifies the temperature-dependent mass-loss behavior associated with sitophilure. The Korsmeyer–Peppas model provided an empirical description of the normalized gravimetric profiles, while the incorporation of activated carbon introduced additional formulation-dependent variations. These findings suggest that the physicochemical characteristics of the polymeric matrix may influence the retention of volatile semiochemicals. However, because unloaded-matrix controls were not available, the kinetic parameters should be interpreted as apparent descriptors of normalized mass loss rather than direct measurements of pheromone release. Further compound-specific analytical investigations are required to establish the mechanisms and quantitative release performance of these materials.

3.2.7 In vivo biological assay with olfactometry

The PCL/sitophilure/activated carbon formulation elicited a significant behavioral response: 70 insects selected the treatment arm and 30 selected the control arm. The chi-square goodness-of-fit test confirmed that the observed distribution differed significantly from an equal 50:50 response ($\chi^2 = 16.00$; df = 1; p = 0.000063; Fig. 8).

The PCL/sitophilure formulation also produced a significant response, with 69 insects selecting the pheromone-containing mat and 31 selecting the control. The distribution differed significantly from the expected 50:50 response ($\chi^2 = 14.44$; df = 1; p = 0.000144; Fig. 8).

Both sitophilure-containing formulations elicited significant attraction of *S. zeamais* under the short-term Y-tube olfactometer conditions, indicating preservation of their biological attractiveness. However, these assays do not quantify sitophilure release or establish long-term field persistence. The thermal and kinetic results indicate formulation-dependent changes in mass-loss behavior, supporting further compound-specific release measurements and field validation. Previous studies have demonstrated prolonged release and field activity of electrospun pheromone dispensers in other insect systems [11, 12, 13].

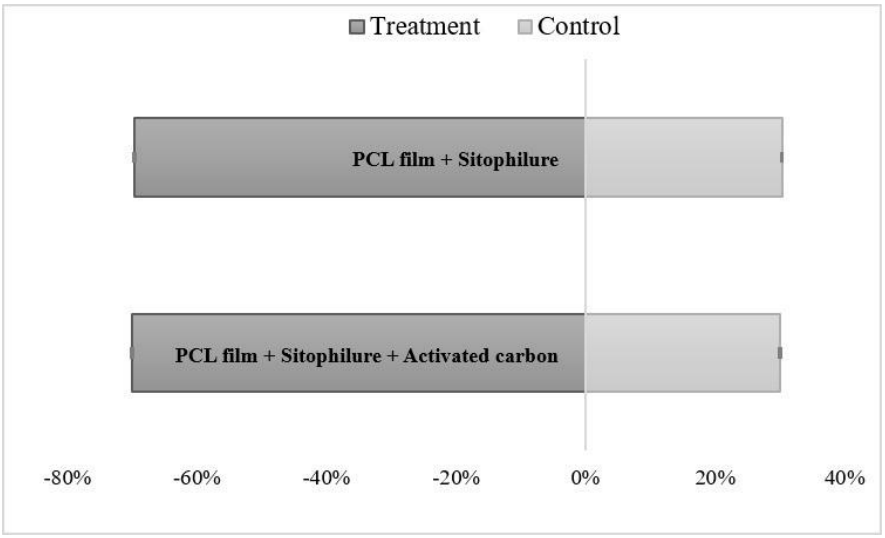

Fig. 8 Behavioral responses of *S. zeamais* in Y-tube olfactometer assays. Treatment: electrospun PCL mats containing sitophilure, with or without activated carbon. Control: electrospun neat PCL mat without sitophilure. Both formulations elicited significant attraction (χ^2 test, $p < 0.001$)

4. Conclusion

Electrospun PCL mats containing sitophilure, with and without activated carbon, were successfully prepared and characterized by complementary spectroscopic, microscopic, thermal, swelling, kinetic, and behavioral analyses. NMR, GC-MS, and FTIR-ATR supported the identity of the synthesized sitophilure, while FTIR-ATR analysis of the mats indicated preservation of the main chemical features of the PCL matrix after incorporation. SEM revealed continuous electrospun microfibers, with formulation-dependent changes in fiber diameter and activated-carbon particles associated with the fibrous structure. TGA and DSC demonstrated that incorporation into PCL altered the thermal behavior of sitophilure and that activated carbon further modified the thermal profile of the ternary formulation. Swelling was strongly dependent on formulation composition and immersion medium, reaching a mean value of 422.1 ± 162.5% for PCL/sitophilure under acidic conditions (pH 4.0), whereas the addition of activated carbon reduced water uptake relative to the binary formulation. Isothermal TGA revealed temperature- and formulation-dependent mass-loss behavior, with the Korsmeyer–Peppas model providing an empirical description of the normalized gravimetric profiles. Because unloaded-matrix controls were unavailable, these results were interpreted as apparent release-related behavior rather than direct quantification of sitophilure release. In Y-tube olfactometer assays, both pheromone-containing formulations elicited statistically significant attraction of *Sitophilus zeamais* relative to the control ($p < 0.001$), demonstrating their biological attractiveness under the experimental conditions. Overall, the findings support the potential of electrospun PCL-based mats as biodegradable carriers for sitophilure in agricultural pest management. Nevertheless, compound-specific release measurements, longer-term stability studies, and field experiments are required to establish dispenser longevity and agronomic performance.

5. Acknowledgments

The authors thank the Federal Institute of Alagoas - IFAL Maceió Campus for the support and assistance of the laboratories in conducting the experiments. They also thank the partnerships involved in the realization of this work, the Federal University of Alagoas - UFAL, the Brazilian Agricultural Research Corporation - Embrapa, the National Council for Scientific and Technological Development - CNPq (Process: 302374/2026-4), the Alagoas State Research Support Foundation - FAPEAL, and the Coordination for the Improvement of Higher Education Personnel - CAPES.

6. References

1. Giles PH (1971) A study of pre-harvest infestation of maize by *Sitophilus zeamais* Motsch. (Coleoptera, Curculionidae) in the Kenya highlands. J Stored Prod Res 7(2):69–83. https://doi.org/10.1016/0022-474X(71)90014-2.

2. Suleiman R, Rosentrater KA, Bern CJ (2015) Evaluation of maize weevils *Sitophilus zeamais* Motschulsky infestation on seven varieties of maize. J Stored Prod Res 64:97–102. https://doi.org/10.1016/j.jspr.2015.09.005.

3. Lemić D, Šimunović K, Pajač Živković I. Harmfulness of two species of weevils (*Sitophilus granarius* L. and Sitophilus zeamais MotschSh.) on different maize hybrids. J Cent Eur Agric. 2021;22(1):178–187. https://doi.org/10.5513/JCEA01/22.1.3113.

4. Conceição ERS, David AMSS, Paraizo EA, Soares LM, Figueiredo JC, Alvarenga CD, Amaro HTR, Custodio DCS, Silva JPM. Qualidade de sementes de milho infestadas com *Sitophilus zeamais* após aplicação de extratos vegetais e terra de diatomácea. Cad Pedagog. 2024;21(13):e10213. https://doi.org/10.54033/cadpedv21n13-102.

5. Potrich M, Alves LFA, Mertz NR, Bonini AK, Silva ERL, Marchese LPC. Seleção e associação de cultivares de milho com *Beauveria bassiana* para o controle de *Sitophilus zeamais* (Coleoptera: Curculionidae). Semina Cienc Agrar. 2010;31(1):5–18. https://doi.org/10.5433/1679-0359.2010v31n1p5.

6. Heuskin S, Verheggen FJ, Haubruge E, Wathelet JP, Lognay G. The use of semiochemical slow-release devices in integrated pest management strategies. Biotechnol Agron Soc Environ. 2011;15(3):459–470. https://popups.uliege.be/1780-4507/index.php?id=7778.

7. Walgenbach CA, Phillips JK, Faustini DL, Burkholder WE. Male-produced aggregation pheromone of the maize weevil, *Sitophilus zeamais*, and interspecific attraction between three Sitophilus species. J Chem Ecol. 1983;9(7):831–841. https://doi.org/10.1007/BF00987808.

8. Kehat M, Anshelevich L, Dunkelblum E, Fraishtat P, Greenberg S. Sex pheromone traps for monitoring the codling moth: effect of dispenser type, field aging of dispenser, pheromone dose and type of trap on male captures. Entomol Exp Appl. 1994;70(1):55–62. https://doi.org/10.1111/j.1570-7458.1994.tb01758.x.

9. Lima RMF, Souza VV. Biodegradable polymers: Application in agriculture and their use as an alternative for environmental protection. Rev Agrogeoamb. 2011;3(2):45–54. https://doi.org/10.1201/9781003230533-21.

10. Xiang HM, Wei XH, Li YR, Zhang BJ, Li M, Ma RY. Electrospun nanofibers as controlled release systems for the combined pheromones of *Grapholita molesta* and *Cydia pomonella*. Pest Management Science. 2025;81(4):2257–2265. https://doi.org/10.1002/ps.8623.

11. Kikionis S, Ioannou E, Konstantopoulou M, Roussis V. Electrospun micro/nanofibers as controlled release systems for pheromones of *Bactrocera oleae* and *Prays oleae*. J Chem Ecol. 2017;43(3):254–262. https://doi.org/10.1007/s10886-017-0831-2.

12. Shangguan W, Xu H, Ding W, Chen H, Mei X, Zhao P, Cao C, Huang Q, Cao L. Nano-Micro Core-Shell Fibers for Efficient Pest Trapping. Nano Lett. 2023;23(24):11809–11817. https://doi.org/10.1021/acs.nanolett.3c03817.

13. Shangguan WJ, Mei XD, Chen HP, Hu S, Xu CL, Wang L, et al. Biodegradable electrospun fibers as sustained-release carriers of insect pheromones for field trapping of Spodoptera litura (Lepidoptera: Noctuidae). Pest Management Science. 2023; 79:4774–4783. https://doi.org/10.1002/ps.7673.

14. Pilli RA, Murta MM, Russowsky D, Boeckelmann MA. Total synthesis of (4SR,5RS)-5-hydroxy-4-methyl-3-heptanone, the racemic form of the aggregation pheromone of *S. orizae* and *S. zeamais*. J Braz Chem Soc. 1991;2(3):121–123. https://doi.org/10.5935/0103-5053.19910026.

15. Shakirzyanova G, Romanova L, Babaev B, Abdukacharov V, Iskandarov T, Gayibova S. Synthesis of a synthetic analogue for the Sitophilus weevil aggregation pheromone and study on its hygienic and toxicological indexes. Acta Agric Slov. 2021;117(2):1–8. https://doi.org/10.14720/aas.2021.117.2.1961.

16. Guimarães AM, Lopes ACO, Nogueira FRZL, Dornelas CB, Freitas JD, Ribeiro AS, Salomão R, Costa LMM. Development of biodegradable PCL nanofiber membranes containing rosehip oil. Rev DELOS. 2026;19(78):109. https://doi.org/10.55905/rdelosv19.n78-109.

17. Damonte G, Cozzani M, Di Lisa D, Pastorino L, Mariani A, Monticelli O. Mechanically-reinforced biocompatible hydrogels based on poly(N-isopropylacrylamide) and star-shaped polycaprolactones. Eur Polym J. 2023;195:112239. https://doi.org/10.1016/j.eurpolymj.2023.112239.

18. Cremasco MA, Nazareno BP. Análise termogravimétrica do óleo essencial de pimenta longa (Piper hispidinervium C. DC.). Acta Amazonica. 2011;41(2):275–278. https://doi.org/10.1590/S0044-59672011000200012.

19. Santos A, García M, Cotes AM, Villamizar L. Efecto de la formulación sobre la vida útil de bioplaguicidas a base de dos aislamientos colombianos de Trichoderma koningiopsis Th003 y Trichoderma asperellum Th034. Rev Iberoam Micol. 2012;29(3):150–156. https://doi.org/10.1016/j.riam.2011.11.002.

20. Korsmeyer RW, Gurny R, Doelker E, Buri P, Peppas NA. Mechanisms of solute release from porous hydrophilic polymers. Int J Pharm. 1983;15(1):25–35. https://doi.org/10.1016/0378-5173(83)90064-9.

21. Ritger PL, Peppas NA. A simple equation for description of solute release I. Fickian and non-Fickian release from non-swellable devices in the form of slabs, spheres, cylinders or discs. J Control Release. 1987;5(1):23–36. https://doi.org/10.1016/0168-3659(87)90034-4.

22. León JG, Estrada-Villegas GM, Olayo-González R, Muñoz EJ, Morales-Corona J, Olayo-Valles R, Martínez-Hernández RC. Caracterización y estudio de liberación de curcumina cargada en microfibras de ácido poliláctico. Rev Fac Cienc. 2020;9(1):125–141. https://doi.org/ 10.15446/rev.fac.cienc.v9n1.81966.

23. Cavalcante M, Costa JG. Considerations on experimental design and the adequacy of using statistical tests in Agricultural Sciences. Diversitas J. 2021;6(4):3706–3723. https://doi.org/10.48017/dj.v6i4.1931.

24. Nazarkina ZK, Stepanova AO, Chelobanov BP, Kvon RI, Simonov PA, Karpenko AA, Laktionov PP. Activated Carbon-Enriched Electrospun-Produced Scaffolds for Drug Delivery/Release in Biological Systems. Int J Mol Sci. 2023;24(7):6713. https://doi.org/10.3390/ijms24076713.

25. Choi S, Raja IS, Selvaraj AR, Kang MS, Park TE, Kim KS, Hyon SH, Han DW, Park JC. Activated carbon nanofiber nanoparticles incorporated electrospun polycaprolactone scaffolds to promote fibroblast behaviors for application to skin tissue engineering. Adv Compos Hybrid Mater. 2023;6:24. https://doi.org/10.1007/s42114-022-00608-x.

26. Medeiros GB, Lima FA, Almeida DS, Guerra VG, Aguiar ML. Modification and Functionalization of Fibers Formed by Electrospinning: A Review. Membranes. 2022;12(9):861. https://doi.org/10.3390/membranes12090861.

27. Bläker C, Muthmann J, Pasel C, Bathen D. Characterization of activated carbon adsorbents – state of the art and novel approaches. ChemBioEng Rev. 2019;6(4):119–138. https://doi.org/10.1002/cben.201900008.

28. Boehm HP. Surface oxides on carbon and their analysis: a critical assessment. Carbon. 2002;40(2):145–149. https://doi.org/10.1016/S0008-6223(01)00165-8.

29. Phillipson K, Hay JN, Jenkins MJ. Thermal analysis FTIR spectroscopy of poly(ε-caprolactone). Thermochim Acta. 2014; 595:74–82. https://doi.org/10.1016/j.tca.2014.08.027.

30. Ruseckaite RA, Jiménez A. Thermal degradation of mixtures of polycaprolactone with cellulose derivatives. Polym Degrad Stab. 2003;81(2):353–358. https://doi.org/10.1016/S0141-3910(03)00106-X.

31. Mohamed AA, Finkenstadt VL, Gordon SH, Biresaw G, Palmquist DE, Rayas-Duarte P. Thermal properties of PCL/gluten bioblends characterized by TGA, DSC, SEM, and infrared-PAS. J Appl Polym Sci. 2008;110(5):3256–3266. https://doi.org/10.1002/app.28914.

32. Morais RM, Santana GM, Lelis RCC, Paes JB (2019) Production of microporous activated carbon with steam prepared from coconut endocarp (Cocos nucifera). Adv For Sci 6(3):699–703. https://doi.org/10.34062/afs.v6i3.6717.

33. Yin M, Zheng S (2005) Ternary thermosetting blends of epoxy resin, poly(ethylene oxide) and poly(ε-caprolactone). Macromol Chem Phys 206:929–937. https://doi.org/10.1002/macp.200400512.

34. Nojima S, Fujimoto M, Kakihira H, Sasaki S (1998) Effects of copolymer composition on the crystallization and morphology of poly(ε-caprolactone)-block-polystyrene. Polym J 30(12):968–975. https://doi.org/10.1295/polymj.30.968.

35. Tabia Z, Akhtach S, Bricha M, El Mabrouk K (2021) Tailoring the biodegradability and bioactivity of green-electrospun polycaprolactone fibers by incorporation of bioactive glass nanoparticles for guided bone regeneration. Eur Polym J 161:110841. https://doi.org/10.1016/j.eurpolymj.2021.110841.

36. Pant HR, Neupane MP, Pant B, Panthi G, Oh HJ, Lee MH, Kim HY (2011) Fabrication of highly porous poly(ε-caprolactone) fibers for novel tissue scaffold via water-bath electrospinning. Colloids Surf B Biointerfaces 88:587–592. https://doi.org/10.1016/j.colsurfb.2011.07.045.

37. Salom C, Nava D, Prolongo MG, Masegosa RM (2006) Poly(ε-caprolactone) + unsaturated isophtalic polyester blends: Thermal properties and morphology. Eur Polym J 42:1798–1810. https://doi.org/10.1016/j.eurpolymj.2006.02.004.

38. Yang X, Zhu B, Dong T, Pan P, Shuai X, Inoue Y (2008) Interactions between an anticancer drug and polymeric micelles based on biodegradable polyesters. Macromol Biosci 8:1116–1125. https://doi.org/10.1002/mabi.200800085.

39. Simão JA, Bellani CF, Branciforti MC (2017) Thermal properties and crystallinity of PCL/PBSA/cellulose nanocrystals grafted with PCL chains. J Appl Polym Sci 134(8):44493. https://doi.org/10.1002/app.44493.